Electron Temperature Measurement by Thomson Scattering in a Low-Aspect-Ratio RFP RELAX

Ryota UEBA, Sadao MASAMUNE, Akio SANPEI, Kosuke UCHIYAMA, Hiroyuki TANAKA, Kanae NISHIMURA, Go ISHII, Ryosuke KODERA, Haruhiko HIMURA, Daniel J. Den HARTOG[1)] and Haruhisa KOGUCHI[2)]

Kyoto Institute of Technology, Kyoto 606-8585, Japan
[1)] University of Wisconsin-Madison, Madison WI 53706-1302, USA
[2)] National Institute for Advanced Industrial Science and Technology, Tsukuba 305-8568, Japan

(Received 8 September 2013 / Accepted 2 January 2014)

A Thomson scattering diagnostic system has been developed for measuring electron temperatures in low-aspect-ratio reversed-field pinch (RFP) plasmas in REversed-field pinch of Low Aspect ratio eXperiment (RELAX). In the range of plasma currents I_p = 50 - 80 kA, the central electron temperature was around 100 eV and, showed a weakly increasing trend as I_p increases. To estimate the central electron pressure p_{e0}, a density calibration was performed from simultaneous measurements with a 104-GHz microwave interferometer. The maximum p_{e0} increased with I_p up to ~ 70 kA to preserve the approximate relation $p_{e0}/B_{\theta a}{}^2$ ~ constant, where $B_{\theta a}$ is the edge poloidal field. In the higher current region, p_{e0} tended to saturate, which may be improved by optimizing minute control of equilibrium in the higher current region.

Keywords: reversed-field pinch, Thomson scattering diagnostic, electron temperature, high-β plasma, RELAX

DOI: 10.1585/pfr.9.1302009

The electron temperature (T_e) is one of the fundamental parameters used to estimate plasma confinement or energy transport properties through electron channels in high-temperature plasmas. Measurements of electron temperature in high-temperature fusion plasmas are most reliably done using the Thomson scattering diagnostic [1]. We have developed a Thomson scattering diagnostic system for the REversed-field pinch of Low Aspect ratio eXperiment (RELAX).

RELAX [2] is a low-aspect-ratio (low-A) reversed-field pinch (RFP) machine (R = 0.5 m, a = 0.25 m, A = 2) for exploring RFP plasma characteristics in the low-A regime, where to date, experiments have rarely been carried out. We have shown that the operational region in (Θ, F) space could be expanded to extremely deep reversal regions in low-A RFP [3], where $\Theta = B_{\theta a}/\langle B_\phi \rangle$ is the pinch parameter, $F = B_{\phi a}/\langle B_\phi \rangle$ is the field reversal parameter, with edge poloidal field $B_{\theta a}$, edge toroidal field $B_{\phi a}$, and average toroidal field $\langle B_\phi \rangle$. Magnetohydrodynamic (MHD) characteristics have been discussed using an axisymmetric equilibrium reconstruction technique and the resultant safety factor profiles. The effects of lowering A on phase locking of the $m = 1$ modes and phase locking to the wall (locked mode) were discussed based on the reconstructed q profiles [4,5]. It is becoming more and more important to address the relationships between these phenomena and such dimensionless parameters as the magnetic Reynolds number S, which characterizes MHD phenomena and requires reliable measurements of the electron temperature.

One of the research objectives in RELAX includes production of high-β RFP plasmas in low-A RFP configurations. Equilibrium analysis has shown that neoclassical RFP equilibrium with a sizable bootstrap fraction exists in RELAX geometry if β values as high as 20% - 30% could be achieved [6] with nested flux surfaces. Here, the definition of β is given by the total beta, $2\mu_0\langle p \rangle / B_{\theta a}{}^2$, and $\langle p \rangle$, the volume-averaged total pressure of electrons and ions. Since bootstrap fraction of 20% - 30% depend strongly on the pressure and electron temperature profiles, their control is also an important issue. Measurement of electron temperature is therefore also quite important for estimating the poloidal beta value.

In this letter, the Thomson scattering diagnostic system for RELAX is described, and electron temperature behavior in RELAX plasmas is presented.

Figure 1 shows the Thomson scattering diagnostic system for RELAX. It mainly consists of a high-power Nd:YAG laser and associated optical elements for beam injection, scattered-light collection optics, and a polychromator for spectrum measurements. The polychormator has been on loan from the MST group at the University of Wisconsin-Madison [7]. In designing the optical layout of laser incidence, we used two reflection mirrors, a prism, and a lens for laser beam focusing. The criterion for the

author's e-mail: ueba12@nuclear.es.kit.ac.jp, masamune@kit.ac.jp

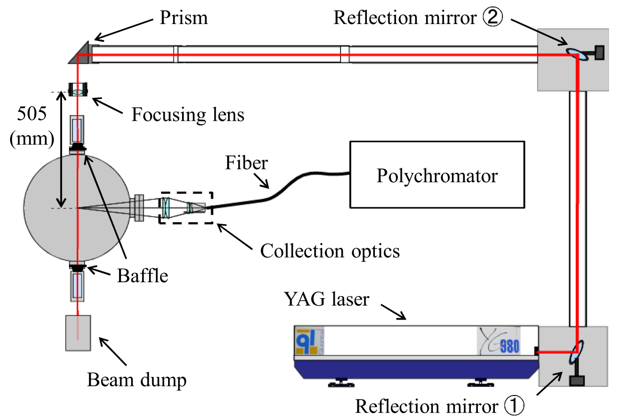

Fig. 1 Schematic of the Thomson scattering diagnostic system for RELAX.

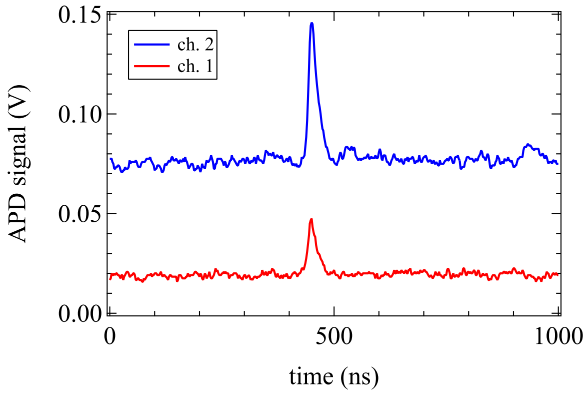

Fig. 3 Example of raw APD signals consisting of scattered light and Bremsstrahlung radiation from channels 1 and 2.

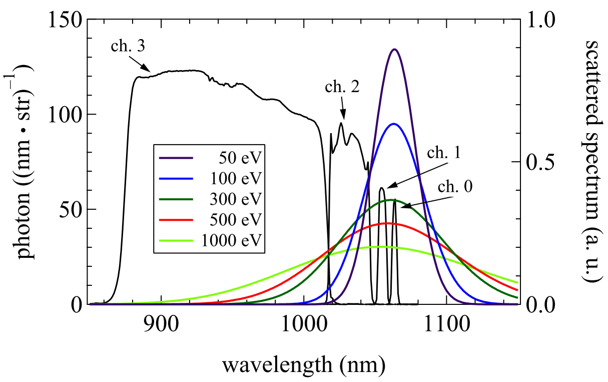

Fig. 2 Typical spectra of Thomson scattered light and instrument function for the four-channel polychromator.

design is to realize the maximum scattering volume along the beam with the minimum plasma volume viewed by the scattered-light collection lens to maximize the S/N ratio, assuming that the major part of the background noise originates from Bremsstrahlung radiation in the plasma. For the present design of our Thomson scattering system, the lower bound on the electron density was estimated to be 3×10^{18} m^{-3}, and the lower bound on T_e was estimated to be 20 - 30 eV. In the polychromator, the scattered light was divided into four-wavelength regions (four channels), and an avalanche photo diode (APD) was used to measure the light intensity for each channel.

The instrument function is a product of the optical transmission of the polychromator system and the quantum efficiency of the detector. Measurements of the polychromator instrument function and absolute calibration for each channel were performed using a quartz-hydrogen DC light source, an absolutely calibrated APD, and InGaAs and Si absolutely calibrated detectors. The calibrations were carried out at the University of Wisconsin, and the detailed calibration procedure is described in [8]. Figure 2 shows the instrument function of the polychromator for each of the four detector channels.

Figure 3 shows an example of raw APD signals, which consist of scattered light and Bremsstrahlung radiation from channels 1 and 2. Since the stray light in channel 0 was too strong to identify the intensity of scattered light, we did not use data from channel 0 in determining the temperature. Despite the strong effect of stray light on the channel 0 signal, its effect on the remaining channels were negligible. In fact, the stray light components in the signals in Fig. 3 are less than one bit, corresponding to 0.83 mV, for both channels. In contrast, the scattered light signal in channel 3 is too small to be distinguished from the Bremsstrahlung component in the temperature region of the present experiments. This agrees with the predicted signal level from the instrument function shown in Fig. 2 for electron temperatures lower than ~ 300 eV.

To determine the scattered light intensity, we subtracted the Bremsstrahlung component according to the following procedure. We defined $t = t_0$ as the time when the APD signal took its maximum value. We then defined two 100-ns time intervals centered at $t = t_0 \pm 150$ ns. The average of the time averaged values over the two time intervals was defined as the Bremsstrahlung component, which was then subtracted from the APD signal to define the scattered light component. The average value of the scattered light at three time points, at $t = t_0$ and at $t_0 \pm 2$ ns, was defined as the scattered light intensity. Using the scattered light intensities from channels 1, 2, and 3, we determined the electron temperature by a best-fit technique. However, in the present temperature regions, this process was almost equivalent to determining the temperature simply from the intensity ratio between channels 1 and 2.

Figure 4 shows the time evolution of the central electron temperature T_{e0} in a standard I_p ~ 50-kA discharge. The plasma current I_p increases to ~ 50 kA in ~ 0.5 ms, while the toroidal loop voltage V_{loop} decreases rapidly to ~ 50 V in ~ 0.7 ms. The flat-topped (or slightly increasing) current phase was maintained up to ~ 2 ms, while V_{loop} decreases gradually down to ~ 25 V. The pinch parameter Θ

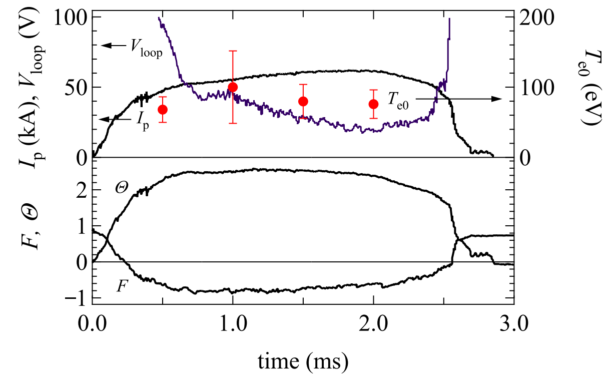

Fig. 4 Time evolution of central electron temperature T_{e0} in typical deep-reversal RFP plasma in RELAX.

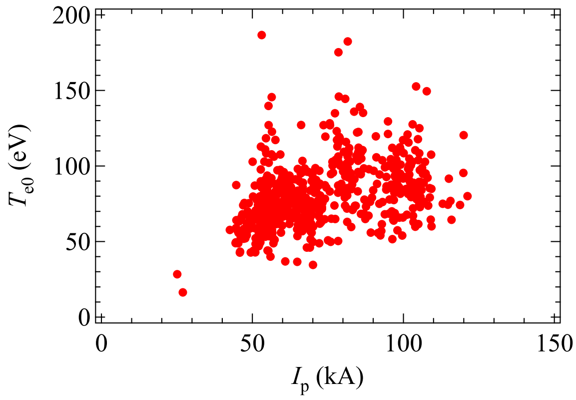

Fig. 5 Relation between central electron temperature T_{e0} and plasma current I_p in RELAX plasmas.

is ~ 2 at I_p = 50 kA, keeping Θ ~ 2.5 during the flat-topped current phase. The field reversal parameter F decreases to ~ −1.0, then increases gradually to ~ −0.5 toward the end of the discharge. The discharge shown in Fig. 4 is categorized as typical for deep-reversal RFP plasmas.

Time evolution of T_{e0} was obtained from shot-by-shot measurements. At each time, T_{e0} is the ensemble average over 20 - 30 identical shots. The error bars shown in Fig. 4 are the standard deviations over these shots. A typical value of T_{e0} is ~ 70 eV at t = 0.5 ms into the discharge, and slightly higher than 100 eV at t = 1.0 ms. Values of T_{e0} remain almost unchanged or only slightly decreases during the flat-topped phase. During the flat-topped phase, V_{loop} decreases gradually, and so does the Ohmic heating power. The evolution of T_{e0} suggests that electron energy transport in the core region remains unchanged, or improves slightly as time passes through the flat-topped phase.

Similar measurements of time evolutions of T_{e0} were carried out in ~ 80-kA RFP discharges, and additional T_{e0} measurements either at t = 0.5 or 1.0 ms were also carried out. These results are summarized in Fig. 5 in which values of T_{e0} are plotted vs. I_p. The general trend is that clusters of data tend to increase with I_p, with small numbers of

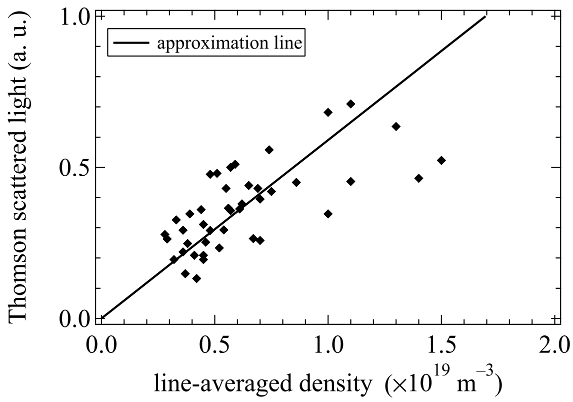

Fig. 6 Relation between total intensity of Thomson scattered light and line-averaged electron density. Straight line is an approximation to the measured relationship.

scattered data in I_p ~ 50 kA and in the high-I_p region. We conclude that we have obtained low-A RFP plasmas with T_{e0} in the 100-eV range and I_p in the range of 60 - 80 kA.

For the electron density, 104-GHz microwave interferometer data were compared with the Thomson scattering data to obtain a density calibration coefficient for Thomson scattering data. The Thomson scattered light intensity was obtained from the electron temperature and scattered light intensities for channels 1 and 2 as follows. Once we determined the electron temperature, we could assign a wavelength spectrum to the Thomson scattered light. By integrating the spectrum over the wavelength, we obtained the total intensity of the scattered light. The relative value can be calculated by estimating the contribution from the wavelength regions for channels 1 and 2, which can also be estimated from the experimental scattered-light intensities from channels 1 and 2. If we compare the total light intensity with simultaneously measured line-averaged electron density, then we can estimate a density calibration coefficient for Thomson scattered light intensity. In Fig. 6, we compare the total intensity of Thomson scattered light with the simultaneously measured line-averaged electron density n_e from the interferometer. In the density region $n_e < 1.6 \times 10^{19}$ m^{-3}, we can identify a linear trend in Fig. 6. Particularly in the high-density region in the figure, scattering may occur because the Thomson scattered light comes from the geometrical center, while the microwave is transmitted through the central vertical chord of the vacuum chamber. Any shift in the magnetic axis from the geometrical center, caused by a Shafranov shift for example, would easily cause a discrepancy in the linear relationship between the local and line-averaged densities. Raman and Rayleigh scattering are yet to be done for calibrating the Thomson scattering system in regard to the density behavior.

In the present analysis, we have approximated the relation shown in Fig. 6 as linear, defining the slope as the calibration coefficient for estimating the central electron

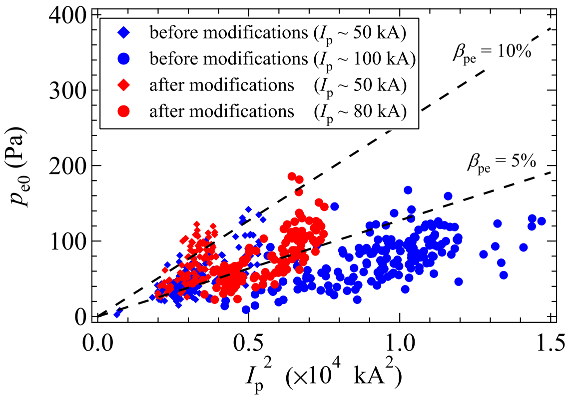

Fig. 7 Relation between central electron pressure p_{e0} and square of the plasma current $I_p{}^2$. The two lines correspond to $p_{e0}/(B_{\theta a}{}^2/2\mu_0)$ = 10% and 5%, respectively.

density n_{e0}. Note that the calibration coefficient includes an uncertainty of 30% which was estimated from the data in the low-density region in Fig. 6. Adopting this calibration procedure, we estimated the central electron pressure $p_{e0} = n_{e0}k_B T_{e0}$, where k_B is the Boltzmann constant. The results are given in Fig. 7, where values of p_{e0} are plotted vs. $I_p{}^2$. The blue and red points in the figure are explained below. The maximum central electron pressure increases with plasma current up to $I_p{}^2 \sim 0.7 \times 10^4$ kA^2 and saturates in the higher current region. In the figure, two lines are drawn to aid the eye. The steep line corresponds to a "central electron poloidal beta" β_{pe} of 10%, where β_{pe} is defined by the ratio of the central electron pressure to the pressure of the edge poloidal field. The results show that the maximum electron pressure in the lower current region ($I_p{}^2 < 0.7 \times 10^4$ kA^2) reaches values corresponding to $\beta_{pe} \sim 10\%$. The other line in Fig. 7 corresponds to β_{pe} of 5%, which indicates that the electron beta value in the saturated region is lower than ~ 5%.

Saturation of electron pressure and thus the lower β_{pe} values in the higher current region appear to be related to both the value of plasma current and equilibrium control. During the course of the Thomson temperature measurements, we modified our passive equilibrium control system to improve the poloidal symmetry of passive control currents. In addition, we installed new windings and power supplies for fine-tuning equilibrium. The red points in Fig. 7 were obtained after these modifications, while the blue points are from before the modifications. In the lower current region, we may identify a slightly higher β_{pe} trend after the modifications. In the higher current region, all the data were obtained before the modifications. The results appear to indicate the importance of minute equilibrium control in achieving high-β plasmas at high current. Optimization of the equilibrium control in high-current region ($I_p \sim 100$ kA) is in progress.

We now make some attempt to compare the present β_{pe} values with those from other RFP experiments. In the initial experiment in MST, values of β_{pe} were reported over a wide range of plasma currents and electron densities in "standard" RFP plasmas [9]. Here "standard" means they did not apply the current profile control technique known as the pulsed poloidal current drive (PPCD). The general trend was that β_{pe} decreased for higher plasma currents, and for higher values of I_p/N at a fixed value of I_p, where N is the line density. The maximum value they achieved was reported to be around 12%. In one of the TPE-RX experiments, an estimated total β_p of 13% was achieved during or right after the PPCD phase [10]. Electrons contributed to about half of this β_p value. The central electron beta values in these experiments were close to the maximum values achieved in RELAX. From the viewpoint of the aspect ratio effect, it would be an important issue to clarify whether any further increase in β_{pe} is possible by only fine-tuning equilibrium in the high-current regime in RELAX.

Recent experiments in MST succeeded in achieving a maximum β_p of 40% by using PPCD in combination with a pellet injection technique, with an energy confinement time of ~ 5 ms; this represents a five-fold improvement in confinement compared to the standard case [11]. It can be estimated that electrons contributed about half of the β_p.

A Thomson scattering diagnostic system has been developed for measuring electron temperatures in low-A RFP plasmas in RELAX. The central electron temperatures occur around 100 eV at I_p of 50 - 80 kA, and they show a weakly increasing trend with I_p. Density calibration was performed from simultaneous measurements with a 104-GHz microwave interferometer, thereby making it possible to estimate the central electron pressure. The maximum central electron pressure increases with I_p to ~ 70 kA to preserve the approximate relation $\beta_{pe} \sim$ constant. In the higher current region, p_{e0} tends to saturate, which could be improved by optimizing minute control of equilibrium.

This work was supported by JSPS KAKENHI Grant Number 22360390, NIFS Collaboration program (NIFS07KOAH022), and JSPS US-Japan Fusion Collaboration program.

[1] I. H. Hutchinson, *Principles of Plasma Diagnostics* (Cambridge Univ. Press, Cambridge) 2nd ed., p. 276 (2002).
[2] S. Masamune *et al.*, J. Phys. Soc. Jpn. **76**, 123501 (2007).
[3] R. Ikezoe *et al.*, Plasma Phys. Control. Fusion **53**, 025003 (2011).
[4] R. Ikezoe *et al.*, Plasma Phys. Control. Fusion **55**, 015005 (2013).
[5] R. Ikezoe *et al.*, J. Phys. Soc. Jpn. **81**, 115001 (2012).
[6] A. Sanpei *et al.*, J. Phys. Soc. Jpn. **78**, 013501 (2009).
[7] J.A. Reusch *et al.*, Rev. Sci. Instrum. **79**, 10E733 (2008).
[8] H.D. Stephens *et al.*, Rev. Sci. Instrum. **79**, 10E734 (2008).
[9] S. Hokin *et al.*, Phys. Fluids B **3**, 2241 (1991).
[10] Y. Yagi *et al.*, Phys. Plasmas **10**, 2925 (2003).
[11] M.D. Wyman *et al.*, Phys. Plasmas **15**, 010701 (2008).